

Ferulic acid encapsulated chitosan-tripolyphosphate nanoparticles attenuate quorum sensing regulated virulence and biofilm formation in *Pseudomonas aeruginosa* PAO1

ISSN 1751-8741
Received on 19th February 2018
Revised 11th May 2018
Accepted on 3rd July 2018
E-First on 22nd August 2018
doi: 10.1049/iet-nbt.2018.5114
www.ietdl.org

Subhaswaraj Pattnaik¹, Subhashree Barik¹, Gangatharan Muralitharan², Siddhardha Busi¹ ✉

¹Department of Microbiology, School of Life Sciences, Pondicherry University, Puducherry-605 014, India

²Department of Microbiology, School of Life Sciences, Bharathidasan University, Tiruchirappalli-620 024, India

✉ E-mail: siddhardha.busi@gmail.com

Abstract: *Pseudomonas aeruginosa* is an opportunistic nosocomial pathogenic microorganism causing majority of acute hospital-acquired infections and poses a serious public health concern. The persistence of bacterial infection can be attributed to the highly synchronised cell-to-cell communication phenomenon, quorum sensing (QS) which regulates the expression of a number of virulence factors and biofilm formation which eventually imparts resistance to the conventional antimicrobial therapy. In this study, the anti-quorum sensing and anti-biofilm potential of ferulic acid encapsulated chitosan-tripolyphosphate nanoparticles (FANPs) was investigated against *P. aeruginosa* PAO1 and compared with native ferulic acid. Dynamic light scattering and transmission electron microscopic analysis confirmed the synthesis of FANPs with mean diameter of 215.55 nm. FANPs showed significant anti-quorum sensing activity by downregulating QS-regulated virulence factors. In addition, FANPs also significantly attenuate the swimming and swarming motility of *P. aeruginosa* PAO1. The anti-biofilm efficacy of FANPs as compared to native ferulic acid was established by light and confocal laser scanning microscopic analysis. The promising results of FANPs in attenuating QS highlighted the slow and sustained release of ferulic acid at the target sites with greater efficacy suggesting its application towards the development of anti-infective agents.

1 Introduction

Pseudomonas aeruginosa is an important nosocomial and opportunistic pathogen causing severe morbidity and mortality in majority of the hospital-acquired infections particularly in the immune-compromised patients [1]. The emergence of multidrug resistance phenomenon in *P. aeruginosa* can be attributed to the extensive and irrational utilisation of traditional antibiotics. In addition, the signs of resistance and biofilm formation in *P. aeruginosa* are due to the highly complex regulatory cell-to-cell communication behaviour termed as quorum sensing (QS). QS in *P. aeruginosa* is well studied with interrelated QS hierarchy such as Las, Rhl and PQS system regulating the coordination of virulence gene expression. According to an estimation, more than 600 genes are regulated by QS circuits with the production of an array of virulence factors such as toxins, proteases and haemolysins [2]. Due to the increasing multidrug resistance phenomenon with concomitant decrease in the efficiency of traditional antimicrobial drugs, considerable interest has been shifted towards developing alternative approach targeting bacterial virulence. In that scenario, bacterial QS has been considered as a plausible therapeutic target to attenuate bacterial virulence and associated biofilm formation, development and maturation [3].

From last few decades a number of synthetic, semi-synthetic chemical moieties were investigated for their QS inhibition potential. However, the extensive use of these compounds and their analogues lead to serious problem of toxicity and lack of bioabsorbability [4]. In this context, natural products from plant as well as microbial origin represent the current drug discovery scenario in the quest for novel anti-infective strategies [5]. In recent years, plant phytoconstituents especially flavonoids, polyphenolic compounds and terpenoids are gaining considerable attention for their QS attenuation properties due to their other therapeutic excellence. In this regard, quercetin (flavonol), zingerone (phenolic compound) and phytol (diterpenes) are some

of the examples of phytoconstituents with potential anti-quorum sensing and anti-biofilm activity [6–8].

Ferulic acid is a common phenolic compound found in many plants and constitutes one of the main components in the polyphenolic compounds. Ferulic acid shows tremendous therapeutic properties with potent antioxidant, antibacterial, anti-viral, anti-inflammatory, anti-cancer, anti-diabetic and cytoprotective properties [9–11]. Though ferulic acid excels in therapeutics, its limitation lies in its bioavailability and pharmacokinetic properties. In this context, investigating an alternative delivery system to counteract the bioavailability issues is gaining importance and nanotechnology provides a strong platform for efficient and targeted delivery with the advantage of controlled and sustained release and capacity to cross biological barriers as compared to the bulk counterparts [12]. Among the nanomaterials used for efficient delivery of drugs, chitosan has received emerging interest due to its physical and chemical properties. Besides, its combination with tripolyphosphate (TPP) not only enhances the entrapment efficiency of the drug but also results in controlled and targeted delivery [13]. Ferulic acid in combination with chitosan was already exploited for improved antioxidant activity than the native materials [14]. Recently, ferulic acid encapsulated chitosan nanoparticles are reported for its anti-biofilm activity against *Candida albicans* biofilm and suggested its efficacy towards the development of novel anti-infectives [15].

In this study, ferulic acid encapsulated chitosan-TPP nanoparticles were synthesised by simple ionic-gelation method, characterised and evaluated for its efficacy in attenuating QS associated virulence and biofilm formation in *P. aeruginosa* PAO1 as compared to the native ferulic acid.

2 Materials and methods

2.1 Chemicals and reagents

Chitosan, low molecular weight (75–85% deacetylation) and pentasodium TPP (technical grade 85%) were procured from Sigma-Aldrich, USA. Ferulic acid and acetic acid glacial, aldehyde free were obtained from Hi media Pvt. Ltd., Mumbai, India.

2.2 Preparation of chitosan and TPP solutions

For the preparation of chitosan solution (0.25% w/v), chitosan flakes were agitated in 1% aqueous solution of glacial acetic acid at ambient room temperature ($25 \pm 2^\circ\text{C}$). Sodium TPP (0.25% w/v) solution was used as cross-linker and prepared by dissolving it in distilled water [16].

2.3 Synthesis of ferulic acid encapsulated chitosan-TPP nanoparticles (FANPs)

FANPs were synthesised by the ionic gelation method. Briefly, ferulic acid was added gradually into chitosan solution (0.25% w/v) under magnetic stirring at ambient temperature for 30–45 min followed by dropwise addition of 0.25 mg/ml of TPP solution in a ratio of 1:5 with respect to chitosan under continuous stirring at 1000 rpm for 30 min to yield FANPs. The suspension of nanoparticles was then centrifuged at 12,000 rpm for 60 min and washed with deionised water (three times) to remove the unloaded compounds [17, 18].

2.4 Physicochemical characterisation of synthesised FANPs

Ultra-violet-visible (UV-Vis) spectroscopic analysis was performed to monitor the formation of FANPs. The UV-Vis absorption spectra were recorded for the reaction mixture over a wavelength range of 200–800 nm using a UV-Vis spectrophotometer. Dynamic light scattering (DLS) was used to measure the mean particle size of synthesised FANPs using particle size analyser (Malvern-Nano Series) at 25°C with scattering angle of 90° . The particle size was described as the mean diameter, the Z-average value. The size and morphology of synthesised FANPs were analysed using high-resolution transmission electron microscope (Jeol/JEM 2100) at an accelerating voltage of 200 kV [15, 16].

2.5 Fourier transform infrared (FTIR) analysis

FTIR spectra of chitosan, ferulic acid and FANPs were recorded to analyse the bonds and functional groups present. The samples were ground thoroughly with potassium bromide (KBr) in ~1:100 sample to KBr ratio to form very fine powder. Then it was compressed to thin pellet and subjected for spectral analysis at the range of 500–4500 cm^{-1} at a resolution of 1 cm^{-1} [19].

2.6 Determination of encapsulation efficiency (EE)

The EE% of FANPs was determined to validate the amount of ferulic acid loaded into the nanoparticle using UV/Vis spectrophotometry (Cary 60 Agilent technology). The supernatant was collected after centrifugation and non-encapsulated ferulic acid was quantified spectrophotometrically at 310 nm using ferulic acid standard curve [15]. The EE (%) was calculated by using the following equation:

$$\text{EE}(\%) = \frac{\text{Total ferulic acid loaded} - \text{Non-encapsulated ferulic acid}}{\text{Total ferulic acid loaded}} \times 100$$

2.7 In-vitro controlled release of ferulic acid

The in-vitro release of ferulic acid from the encapsulated FANPs was studied to evaluate the controlled and sustained release of

ferulic acid. The dried nanoparticles were suspended in phosphate buffered saline (PBS, 0.15 M, pH 7.4) at a concentration of 1.0 mg/ml of nanoparticles and incubated at 37°C . At predetermined time intervals (4 h) up to 24 h, samples were withdrawn and centrifuged at 8000 rpm for 10 min to separate the released ferulic acid. The supernatant was used for analysis by UV-Vis spectrophotometry at 310 nm following the entrapment efficiency procedure outlined above to quantify the ferulic acid content [19]. The percentage of ferulic acid released was determined from the following equation:

$$\text{Release}(\%) = \frac{\text{Released ferulic acid from nanoparticle}}{\text{Total amount of ferulic acid in nanoparticle}} \times 100$$

2.8 Anti-quorum sensing activity of FANPs

2.8.1 Determination of minimum inhibitory concentration (MIC): The MIC for the native ferulic acid and FANPs were determined as per the guidelines of Clinical and Laboratory Standards Institute [20]. Briefly, overnight *P. aeruginosa* PAO1 culture (adjusted to 0.5 McFarlands standard corresponds to 1.5×10^8 CFU/ml) was added to freshly prepared LB medium supplemented with the native ferulic acid and FANPs to attain the final concentrations ranging from 32 to 1000 $\mu\text{g/ml}$ and incubated at 37°C for 24 h. All further assays were carried out using the 0.5 McFarland standard (1.5×10^8 CFU/ml).

2.8.2 Pyocyanin inhibition assay: The pyocyanin pigment production by *P. aeruginosa* PAO1 on treatment with sub-MIC concentrations of ferulic acid and FANPs was measured by the method described by Luo *et al.* [20] with slight modification. Briefly, overnight *P. aeruginosa* PAO1 with ferulic acid and FANPs was kept for incubation for 16–18 h. After the incubation, the culture was pelleted by centrifugation at 13,000 rpm for 10 min. The cell-free supernatant containing the pyocyanin was then extracted with 0.6 ml of chloroform. The organic layer was reextracted with 0.2 ml of 0.2 M HCl. The absorbance of the supernatant was measured at 520 nm.

2.8.3 Growth curve analysis: Overnight culture of *P. aeruginosa* PAO1 was inoculated in freshly prepared LB broth supplemented with sub-MIC concentration (500 $\mu\text{g/ml}$) of ferulic acid and FANPs. The treated culture was incubated at 37°C under 100 rpm in a rotatory shaker. The cell density was measured in UV-Vis spectrophotometer at every 2 h interval up to 24 h [21].

2.8.4 LasA staphylolytic activity: The LasA staphylolytic activity was measured to determine the ability of *P. aeruginosa* PAO1 to lyse *Staphylococcus aureus* cells. Briefly, 30 ml of an overnight *S. aureus* culture was boiled for 10 min and then centrifuged for 10 min at 13,000 rpm. The resulting pellet was resuspended in 10 mM Na_2PO_4 (pH 4.5). Overnight *P. aeruginosa* PAO1 on treatment with ferulic acid and FANPs were centrifuged at 13,000 rpm for 10 min. A 100 μl aliquot of *P. aeruginosa* test supernatant was added to 900 μl of the *S. aureus* suspension. Optical density of the mixture (OD_{600}) was determined and percentage of inhibition in staphylolytic activity was determined [22].

2.8.5 Anti-motility assay: For swimming assay, overnight culture of *P. aeruginosa* PAO1 was point inoculated at the centre of the swimming medium consisting of 1% tryptone, 0.5% NaCl and 0.3% agar with various concentrations (250 and 500 $\mu\text{g/ml}$) of ferulic acid and FANPs. For swarming assay, test bacteria were point inoculated at the centre of the swarming medium (1% peptone, 0.5% NaCl, 0.5% agar and 0.5% of sterilised D-glucose) containing sub-MIC concentrations of ferulic acid and FANPs (250 and 500 $\mu\text{g/ml}$). The plates were incubated at 37°C for 16–18 h and swimming and swarming migration of *P. aeruginosa* PAO1 was evaluated [23].

2.9 Anti-biofilm efficacy of ferulic acid and FANPs against *P. aeruginosa* PAO1 biofilm

2.9.1 Biofilm formation assay (microtitre plate method): For biofilm quantification, a microtitre plate based method was followed as per the protocol given by Zhang *et al.* [24] with slight modification. Briefly, ferulic acid and FANPs treated *P. aeruginosa* PAO1 culture was incubated overnight in a microtitre plate. After 24 h of incubation, biofilms formed by bacterial culture were stained with crystal violet (0.1% w/v) for 20 min. After washing with water, the liquid was discarded from the wells and the material that remained fixed to the polystyrene (containing biofilm) was washed with PBS (thrice). Crystal violet bound to biofilm was dissolved in absolute ethanol at 37°C for 30 min. The absorbance of the suspension was measured at 540 nm.

2.9.2 Exopolysaccharides (EPS) inhibition assay: The role of ferulic acid and FANPs on production of EPS by *P. aeruginosa* PAO1 was determined according to the method described by Rasamiravaka *et al.* [25]. Briefly, *P. aeruginosa* PAO1 was incubated for 18 h with ferulic acid and FANPs (250 and 500 µg/ml). After incubation, the culture was centrifuged at 10,000 rpm for 15 min. The pellets were resuspended in high salt buffer and recentrifuged at 10,000 rpm for 30 min and 3 volume of 95% ethanol were added to it, followed by overnight incubation at 4°C. After incubation, the suspension was recentrifuged and the precipitate was resuspended in deionised water. Equal volume of 5% phenol was added to the extract followed by addition of 2.5 ml of H₂SO₄. Then, the absorbance was measured at OD₄₉₀ in a microplate reader.

2.9.3 Rhamnolipids inhibition assay: For rhamnolipids extraction, *P. aeruginosa* PAO1 was grown at 37°C with agitation at 100 rpm for 18 h in LB medium supplemented with ferulic acid and FANPs. Bacterial cultures were centrifuged (10,000 rpm, 5 min) and 1 ml of cell-free supernatant was mixed with 1 ml of ethyl acetate and vigorously vortexed. After phase separation the upper rhamnolipid-containing phase was transferred to a new reaction tube. This procedure was repeated three times. Finally, the organic solvent was removed by evaporation. Rhamnolipids were quantified by a methylene-blue-based method as described by Rasamiravaka *et al.* [25] with some modification.

2.9.4 Cell surface hydrophobicity assay: Cell surface hydrophobicity was determined by estimating the percentage of cells transferred from an aqueous phase to an organic one, following the protocol described by Garcia-Lara *et al.* [26]. Briefly, *P. aeruginosa* PAO1 cultures with and without ferulic acid and FANPs were grown in LB medium, centrifuged at 13,000 rpm for 2 min and the cell pellet was washed twice with PUM buffer [2.22 g of potassium phosphate trihydrate, 7.26 g of monobasic potassium phosphate, 1.8 g of urea and 0.2 g of magnesium sulphate heptahydrate/litre (pH 7.1)]. The cells were then resuspended in 1 ml of PUM buffer, 100 µl were taken to determine the initial cell density in the aqueous phase and 400 µl of hexadecane (Sigma) were added to the 900 µl of remaining PUM suspended cells, the mixtures were then vortexed thoroughly for 5 min. The aqueous phase was then removed and the OD₆₀₀ was measured to determine the cell density that remained in the aqueous phase. The percentage of cell surface hydrophobicity was determined using the formula

$$\text{Cell surface hydrophobicity (\%)} = \frac{\text{Initial cell density} - \text{final cell density}}{\text{initial cell density}} \times 100$$

2.9.5 Microscopic analysis of *P. aeruginosa* PAO1 biofilms: To find out the impact of ferulic acid and FANPs on the biofilm forming ability of *P. aeruginosa* PAO1, the biofilm architecture was examined microscopically on treatment with sub-MIC concentrations of ferulic acid and FANPs. For light

microscopic analysis, biofilms were grown on glass slides submerged with tryptic soy broth in 24-well microtitre plate, and incubated at 37°C for 24 h. Following incubation, the glass slides were washed with carbinol and stained with 0.1% crystal violet. The glass slides were dipped in water for removal of extra stain and observed under microscope at 40× magnification [27]. For confocal laser scanning microscope (CLSM) analysis, overnight *P. aeruginosa* PAO1 culture was inoculated into LB broth supplemented with native ferulic acid and FANPs and incubated for 24 h in a 12-well microtitre plate and coverslips were dipped into it. After incubation, the coverslips were transferred onto slides. The slides were kept for air drying for 2–3 min. The slides were stained with acridine orange and kept for 5 min and observed under CLSM at 20× magnification [28].

2.10 Statistical analysis

All the experiments were conducted in triplicate ($n=3$). All the results were presented as mean±standard deviation. One-way analysis of variance followed by the Tukey–Kramer multiple comparison test (Q -test) was used to determine significant differences at varied level of significance as compared to control and native ferulic acid. For statistical analysis, $P<0.05$ was considered significant [15].

3 Results and discussion

3.1 Synthesis of FANPs

Ferulic acid was encapsulated into chitosan biopolymer where TPP was used as a crosslinker, in order to synthesise FANPs. The nanoparticle was successfully formed by the electrostatic interaction between deacetylated chitosan (which have positively charged $-\text{NH}_2$ group) and TPP (having negatively charged phosphate group).

3.2 Physico-chemical characterisation of synthesised FANPs

UV–Vis spectroscopic analysis showed the formation of FANPs with a characteristic change in the SPR pattern as compared to native ferulic acid and chitosan. The DLS analysis confirmed the formation and size distribution of FANPs. The size of FANPs, analysed by DLS showed a Z-average value of 215.55 nm (Fig. 1a). The FANPs dispersion showed a polydispersity index of 0.272. The transmission electron microscopic (TEM) image presented in Fig. 1b showed predominantly anisotropic FANPs with approximate size of 215 nm (Fig. 1b). The size of the ferulic acid encapsulated chitosan nanoparticles observed in the present study was in agreement with the previous results [29].

3.3 FTIR spectrophotometer analysis

In order to confirm the successful formation of FANPs, FTIR studies were carried out. The presence of similar kind of functional group in FANPs in comparison to native ferulic acid and chitosan signifies that ferulic acid was successfully encapsulated into chitosan carrier where TPP act as crosslinker. The FTIR spectra of chitosan have the peaks located at 3463.2, 2880.7, 1642.4, 1361.4 and 1101.1 which correspond to O–H stretch for alcohols, C–H stretch alkane, $-\text{C}\equiv\text{C}-$, C–H rock, alkanes and C–N stretch for aliphatic amines, respectively (Fig. 2). The successful loading of ferulic acid to chitosan carrier was identified by the introduction of a new peak, i.e. at 1686.3 which corresponds to aldehyde (C=O) stretch which was present in both ferulic acid as well as FANPs. The FTIR spectra of FANPs inferred the presence of similar functional groups to that of ferulic acid and chitosan with slight band shifting indicating the encapsulation of ferulic acid on the chitosan-TPP nanoparticles. Similar shift in the FTIR spectrum was reported earlier for kaemferol loaded chitosan nanoparticles [30].

3.4 EE and in-vitro drug release studies

The EE was measured with the help of using a standard curve of ferulic acid. The EE (%) of ferulic acid to chitosan carrier was

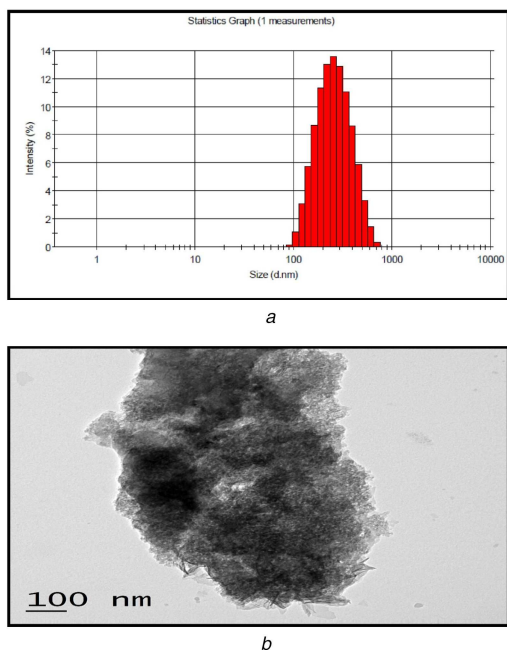


Fig. 1 Size, morphology and distribution of ferulic acid encapsulated chitosan nanoparticles

(a) DLS analysis of FANPs showing the mean diameter of nanoparticles (215.55 nm), (b) TEM image of FANPs showing spherical shape of nanoparticles with a diameter of 215.55 nm

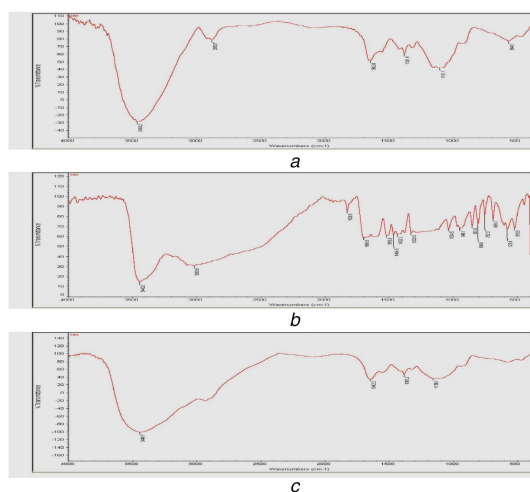


Fig. 2 FTIR analysis

(a) Ferulic acid, (b) Chitosan, (c) FANPs, recorded in the range of 500–4500 cm^{-1} at a resolution of 1 cm^{-1} showing the shift of identical absorption peaks corresponding to change in chemical groups during the encapsulation of ferulic acid into chitosan nanoparticles

observed to be $67.34 \pm 4.09\%$. The in-vitro drug release profile showed that 34% drug was released in the time interval of 12 h in the initial burst. After that $\sim 67\%$ drug was released in the next 12 h. From the size analysis study and observance of more than 65% EE confirmed that nanoparticles were synthesised and loaded into the chitosan-TPP carrier successfully. This result suggested a slow and sustained release of the targeted drug from the encapsulated nanoparticles. In previously reported studies of delivery of phytochemicals by using PLGA nanoparticles, the release studies showed $\sim 20\text{--}50\%$ release of drugs in a span of 24 h [31].

3.5 Anti-quorum sensing activity of FANPs

3.5.1 Determination of MIC and sub-MIC: The MIC of ferulic acid and FANPs against *P. aeruginosa* PAO1 was found to be 1000 $\mu\text{g/ml}$ where the growth and cell density were significantly inhibited as evident from the absence of turbidity. Hence, sub-MIC

concentrations of 250 and 500 $\mu\text{g/ml}$ (i.e. 1/2 and 1/4 MIC, respectively) were used for further activities.

3.5.2 Pyocyanin inhibition assay: Pyocyanin is an important virulence factor produced by *P. aeruginosa* PAO1 and is regulated by Rhl QS system. Pyocyanin plays a critical role in altering the host immune system by generating reactive oxygen species and it has profound importance in the development of acute and persistent respiratory infections [32]. In this study, pyocyanin production was significantly decreased with the increasing sub-MIC concentrations of FANPs as well as native compound ferulic acid. FANPs significantly exhibited 74.85 ± 4.83 and $89.47 \pm 3.16\%$ of inhibition as compared to 50.29 ± 2.81 and $70.17 \pm 6.62\%$ inhibition in case of native ferulic acid at 250 and 500 $\mu\text{g/ml}$, respectively (Fig. 3a). In previously studied reports, the presence of sub-MIC levels of baicalein attenuated the production of pyocyanin up to 69.87% [20].

3.5.3 Growth curve analysis: From the growth curve assay, sub-MIC concentration (500 $\mu\text{g/ml}$) of ferulic acid and FANPs treated *P. aeruginosa* PAO1 exhibited normal growth like that of the untreated control but with slow growth rate as compared to control (Fig. 3b). The result was in accordance to the earlier report suggesting the anti-quorum sensing property instead of bactericidal properties [20].

3.5.4 LasA staphylolytic activity: The QS gene expression in *P. aeruginosa* has interconnection with other signalling regulatory systems which respond to various environmental signals. The virulence factor, LasA protease is under the control of the *lasI-lasR* system. This protease has inhibitory effect on the growth of *S. aureus*, which was significantly reduced on treatment with sub-MIC concentrations of both ferulic acid and FANPs [22]. A significant decrease in LasA staphylolytic activity was observed compared to that of the control when *P. aeruginosa* test supernatant was grown on treatment with sub-MIC concentrations of FANPs and ferulic acid (Table 1).

3.5.5 Anti-motility assay: The flagellar mediated swimming and pili mediated swarming motility of *P. aeruginosa* PAO1 play a crucial role in biofilm formation, development and maturation. The presence of sub-MIC concentration (500 $\mu\text{g/ml}$) of ferulic acid and FANPs significantly altered the swimming and swarming motility of *P. aeruginosa* PAO1 suggesting its role in biofilm disruption which is in accordance with the previous report (Fig. 4) [24].

3.6 Anti-biofilm efficacy of FANPs

3.6.1 Biofilm formation assay (MTP method): The sub-MIC concentrations of ferulic acid and FANPs exhibited significant reduction in biofilm formation as compared to untreated control in a concentration-dependent manner. On treatment with sub-MIC concentrations of FANPs, the reduction in biofilm formation were 67.41 ± 4.13 and $84.33 \pm 3.11\%$ at 250 and 500 $\mu\text{g/ml}$ which were significantly higher than the native ferulic acid (Table 1). The present result was in accordance to the earlier report depicting the biofilm disruption potential of gum Arabic capped silver nanoparticles [33].

3.6.2 EPS inhibition assay: The production of EPS also plays an important role in formation and development of biofilm [25]. In this study, the production of EPS on treatment with sub-MIC concentrations of FANPs and native ferulic acid was significantly altered suggesting the efficacy of FANPs and ferulic acid in inhibition of biofilm formation and development. Table 1 shows the concentration-dependent inhibition of EPS production by *P. aeruginosa* PAO1 on treatment with sub-MIC concentrations of ferulic acid and FANPs. At 500 $\mu\text{g/ml}$ the reduction in EPS production observed were 74.07 ± 5.23 and $61.37 \pm 4.51\%$ for FANPs and native ferulic acid, respectively.

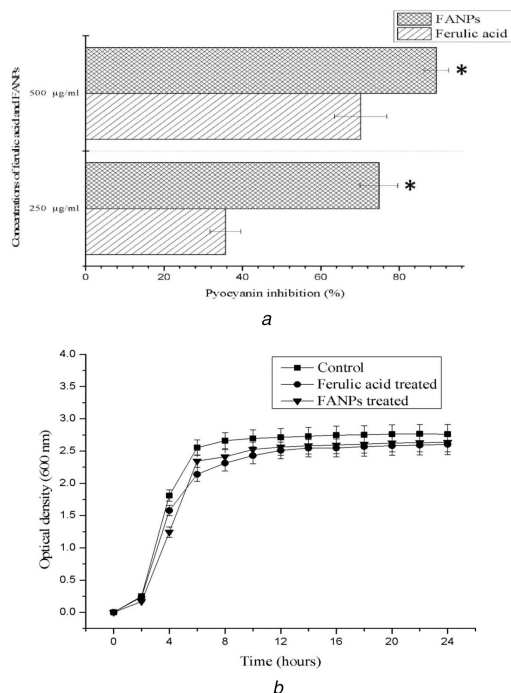


Fig. 3 Effect of sub-MIC concentrations (250, 500 µg/ml) of ferulic acid and FANPs on

(a) Pyocyanin production in *P. aeruginosa* PAO1, (b) Growth curve of *P. aeruginosa* PAO1 on supplementation of native ferulic acid and FANPs (500 µg/ml) as compared to the untreated control

Table 1 Effect of sub-MIC concentrations (250 and 500 µg/ml) of ferulic acid and FANPs on LasA staphylolytic activity and production of rhamnolipids, EPS and biofilm by *P. aeruginosa* PAO1

Concentration, µg/ml	QS inhibitory activity	Percentage of inhibition, %	
		Ferulic acid	FANPs
250	LasA staphylolytic assay	32.44 ± 4.02	51.45 ± 2.53
	biofilm formation assay (MTP)	51.35 ± 3.51	67.41 ± 4.13
	EPS inhibition assay	45.61 ± 3.46	57.48 ± 3.74
	Rhamnolipids inhibition assay	37.11 ± 2.26	55.26 ± 3.65
500	LasA staphylolytic assay	48.16 ± 2.67	63.24 ± 3.07
	biofilm formation assay (MTP)	68.58 ± 4.18	84.33 ± 3.11
	EPS inhibition assay	61.37 ± 4.51	74.07 ± 5.23
	Rhamnolipids inhibition assay	53.09 ± 2.95	73.55 ± 4.58

3.6.3 Rhamnolipids inhibition assay: The production of rhamnolipids by *P. aeruginosa* PAO1 has a greater influence on biofilm formation and development. A significant and concentration-dependent inhibition of production of rhamnolipids was observed when *P. aeruginosa* PAO1 was treated with sub-MIC concentrations of ferulic acid and FANPs (Table 1). In this study, on treatment with sub-MIC concentration (500 µg/ml) of FANPs and ferulic acid, 73.55 and 53.09% of reduction in rhamnolipids production was observed as compared to the untreated control. The result of FANPs was significantly higher than the earlier report. The potential role of FANPs in inhibiting the production of rhamnolipids could be attributed to its role in governing the QS-regulated *rhlAB* operon encoding the enzymes responsible for rhamnolipids biosynthesis [34, 35].

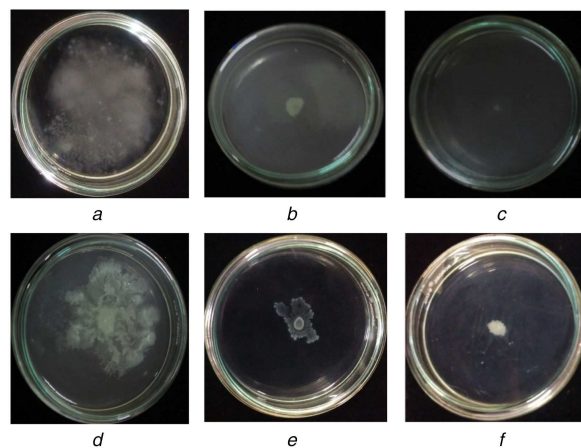


Fig. 4 Swimming and swarming motility

(a) Untreated control swimming plate, (b) Swimming motility of native ferulic acid treated *P. aeruginosa* PAO1, (c) Swimming motility of FANPs treated *P. aeruginosa* PAO1, (d) Untreated control swarming plate, (e) Swarming motility of native ferulic acid treated *P. aeruginosa* PAO1, (f) Swarming motility of FANPs treated *P. aeruginosa* PAO1

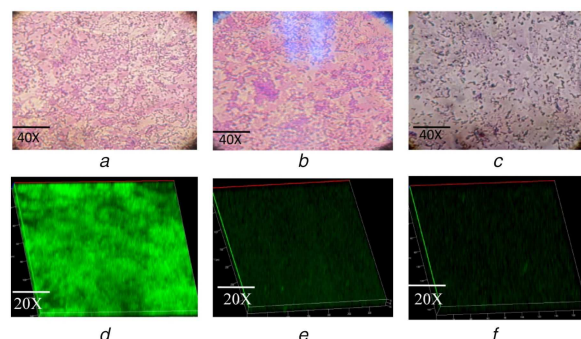


Fig. 5 Microscopic analysis of *P. aeruginosa* PAO1 biofilm

(a) Light microscopic observation of biofilm of untreated control, (b) Light microscopic observation of biofilm treated with ferulic acid, (c) Light microscopic observation of biofilm treated with FANPs, (d) CLSM image of biofilm of untreated control, (e) CLSM image of biofilm treated with ferulic acid, (f) CLSM image of biofilm treated with FANPs

3.6.4 Cell surface hydrophobicity assay: Cell surface hydrophobicity assay inferred the potential of sub-MIC concentrations of ferulic acid and FANPs in decreasing the hydrophobicity of bacterial cells as compared to untreated control. The hydrophobicity percentage of 16.94 ± 2.43 and 35.38 ± 2.6 on treatment with 500 µg/ml of FANPs and ferulic acid, respectively, suggested its role in altering the ability of *P. aeruginosa* PAO1 to form biofilm [26].

3.6.5 Microscopic observation of biofilms: The light microscopic analysis of the biofilm formed by *P. aeruginosa* PAO1 showed visible clumping with complex morphology of the biofilm architecture which was significantly altered on treatment with sub-MIC concentration (500 µg/ml) of FANPs and native ferulic acid suggesting its efficacy in attenuating the antibiotic-resistant biofilm formation and development (Fig. 5) [27]. The visual observation of biofilm disruption potential of FANPs and ferulic acid was further validated by CLSM analysis. The results suggested the altered biofilm architecture with significant reduction in biofilm formation in the treated sample as compared to the clumped and complex biofilm architecture in the untreated control [8].

The results from the present study suggested the efficacy of FANPs in QS attenuation and reduced biofilm formation as compared to the native ferulic acid suggesting the efficacy of nanocarriers in attenuating the QS-controlled virulence factors and biofilm formation due to its slow, sustained and target specific release of ferulic acid at the target sites with a long-term activity in comparison to its native form.

4 Conclusion

In this study both ferulic acid and synthesised FANPs showed potential anti-quorum sensing and biofilm inhibitory activity. As compared to native ferulic acid, the attenuation efficacy of FANPs was found to be significantly higher suggesting the role of a biocompatible nanocarrier system for effective targeting of the virulence with slow and controlled release of encapsulated drugs. The slow and sustained release of drugs from FANPs suggested its persistence to be used as effective QS inhibitor. Owing to tremendous potential in QS inhibition in the present study, FANPs have a great perspective to be used as QS inhibitor against other pathogenic bacteria in the near future.

5 Acknowledgment

The authors thank the Central Instrumentation Facilities (CIF), Pondicherry University for providing DLS and FTIR analysis. They also thank Sophisticated Test and Instrumentation Centre (STIC), Cochin, India for providing TEM analysis.

6 References

- [1] Swatton, J.E., Davenport, P.W., Maunders, E.A., et al.: 'Impact of azithromycin on the quorum sensing-controlled proteome of *Pseudomonas aeruginosa*', *PLoS ONE*, 2016, **11**, (1), p. e0147698
- [2] Zeng, J., Zhang, N., Huang, B., et al.: 'Mechanism of azithromycin inhibition of HSL synthesis in *Pseudomonas aeruginosa*', *Sci. Rep.*, 2016, **6**, p. 24299
- [3] Chang, C., Krishnan, T., Wang, H., et al.: 'Non-antibiotic quorum sensing inhibitors acting against N-acyl homoserine lactone synthase as druggable target', *Sci. Rep.*, 2014, **4**, p. 7245
- [4] Kalia, M., Yadav, V.K., Singh, P.K., et al.: 'Effect of cinnamon oil on quorum sensing- controlled virulence factors and biofilm formation in *Pseudomonas aeruginosa*', *PLoS ONE*, 2015, **10**, (8), p. e0135495
- [5] Silva, L.N., Zimmer, K.R., Macedo, A.J., et al.: 'Plant natural products targeting bacterial virulence factors', *Chem. Rev.*, 2016, **116**, pp. 9162–9236
- [6] Pejcin, B., Ciric, A., Glamoclija, J., et al.: 'In vitro anti-quorum sensing activity of phytol', *Nat. Prod. Res.*, 2015, **29**, (4), pp. 374–377
- [7] Kumar, L., Chhibber, S., Kumar, R., et al.: 'Zingerone silences quorum sensing and attenuates virulence of *Pseudomonas aeruginosa*', *Fitoterapia*, 2015, **102**, pp. 84–95
- [8] Ouyang, J., Sun, F., Feng, W., et al.: 'Quercetin is an effective inhibitor of quorum sensing, biofilm formation and virulence factors in *Pseudomonas aeruginosa*', *J. Appl. Microbiol.*, 2016, **120**, pp. 966–974
- [9] Merlin, J.P.J., Prasad, N.R., Shibli, S.M.A., et al.: 'Ferulic acid loaded poly-D,L-lactide-co-glycolide nanoparticles: systematic study of particle size, drug encapsulation efficiency and anticancer effect in non-small cell lung carcinoma cell line *in vitro*', *Biomed. Prevent.*, 2012, **2**, pp. 69–76
- [10] Trombino, S., Cassano, R., Ferrarelli, T., et al.: 'Trans-ferulic acid-based solid lipid nanoparticles and their antioxidant effect in rat brain microsomes', *Colloids Surf. B, Biointerfaces*, 2013, **109**, pp. 273–279
- [11] Thakkar, A., Chenreddy, S., Wang, J., et al.: 'Ferulic acid combined with aspirin demonstrates chemopreventive potential towards pancreatic cancer when delivered using chitosan-coated solid-lipid nanoparticles', *Cell. Biosci.*, 2015, **5**, p. 46
- [12] Babu, V.N., Kannan, S.: 'Enhanced delivery of baicalin using cinnamaldehyde cross-linked chitosan nanoparticle inducing apoptosis', *Int. J. Biol. Macromol.*, 2012, **51**, pp. 1103–1108
- [13] Hashad, R.A., Ishak, R.A.H., Geneidi, A.S., et al.: 'Methotrexate loading in chitosan nanoparticles at a novel pH: response surface modeling, optimization and characterization', *Int. J. Biol. Macromol.*, 2016, **91**, pp. 630–639
- [14] Woranuch, S., Yoksan, R., Akashi, M.: 'Ferulic acid-coupled chitosan: thermal stability and utilization as an antioxidant for biodegradable active packaging film', *Carbohydr. Polym.*, 2015, **115**, pp. 744–751
- [15] Panwar, R., Pemmaraju, S.C., Sharma, A.K., et al.: 'Efficacy of ferulic acid encapsulated chitosan nanoparticles against *Candida albicans* biofilm', *Microb. Pathog.*, 2016a, **95**, pp. 21–31
- [16] Woranuch, S., Yoksan, R.: 'Preparation, characterization and antioxidant property of water-soluble ferulic acid grafted chitosan', *Carbohydr. Polym.*, 2013, **96**, pp. 495–502
- [17] Lai, P., Daear, W., Lobenberg, R., et al.: 'Overview of the preparation of organic polymeric nanoparticles for drug delivery based on gelatine, chitosan, poly (D,L-lactide-co-glycolic acid) and polyalkylcyanoacrylate', *Colloids Surf. B, Biointerfaces*, 2014, **118**, pp. 154–163
- [18] Panwar, R., Sharma, A.K., Kaloti, M., et al.: 'Characterization and anticancer potential of ferulic acid-loaded chitosan nanoparticles against ME-180 human cervical cancer cell lines', *Appl. Nanosci.*, 2016b, **6**, pp. 803–813
- [19] Rejinold, N.S., Muthunayanan, M., Muthuchelian, K., et al.: 'Saponin-loaded chitosan nanoparticles and their cytotoxicity to cancer cell lines *in vitro*', *Carbohydr. Polym.*, 2011, **84**, pp. 407–416
- [20] Luo, J., Kong, J., Dong, B., et al.: 'Baicalin attenuates the quorum sensing-controlled virulence factors of *Pseudomonas aeruginosa* and relieves the inflammatory response in *P. aeruginosa*-infected macrophages by downregulating the MAPK and NFκB signal-transduction pathways', *Drug. Des. Dev. Ther.*, 2016, **10**, pp. 183–203
- [21] Cady, N.C., McKean, K.A., Behnke, J., et al.: 'Inhibition of biofilm formation, quorum sensing and infection in *Pseudomonas aeruginosa* by natural products-inspired organosulfur compounds', *PLoS ONE*, 2012, **7**, (6), p. e38492
- [22] Alasil, S.M., Omar, R., Ismail, S., et al.: 'Inhibition of quorum sensing-controlled virulence factors and biofilm formation in *Pseudomonas aeruginosa* by culture extract from novel bacterial species of *Paenibacillus* using a rat model of chronic lung infection', *Int. J. Bacteriology*, 2015, **2015**, Article ID: 671562
- [23] Packiavathy, I.A.S.V., Agilandeswari, P., Musthafā, K.S., et al.: 'Antibiofilm and quorum sensing inhibitory potential of *Cuminum cyminum* and its secondary metabolite methyl eugenol against gram negative bacterial pathogens', *Food. Res. Int.*, 2012, **45**, pp. 85–92
- [24] Zhang, J., Rui, X., Wang, L., et al.: 'Polyphenolic extract from *Rosa rugosa* tea inhibits bacterial quorum sensing and biofilm formation', *Food. Cont.*, 2014, **42**, pp. 125–131
- [25] Rasamiravaka, T., Vandeputte, O.M., Pottier, L., et al.: '*Pseudomonas aeruginosa* biofilm formation and persistence, along with the production of quorum sensing-dependent virulence factors, are disrupted by a triterpenoid coumarate ester isolated from *Dalbergia trichocarpa*, a tropical legume', *PLoS ONE*, 2015, **10**, (7), p. e0132791
- [26] Garcia-Lara, B., Saucedo-Mora, M.A., Roldan-Sanchez, J.A., et al.: 'Inhibition of quorum-sensing-dependent virulence factors and biofilm formation of clinical and environmental *Pseudomonas aeruginosa* strains by ZnO nanoparticles', *Lett. Appl. Microbiol.*, 2015, **61**, pp. 299–305
- [27] Sivaranjani, M., Gowrishankar, S., Kamaladevi, A., et al.: 'Morin inhibits biofilm production and reduces the virulence of *Listeria monocytogenes*—An *in vitro* and *in vivo* approach', *Int. J. Food. Microbiol.*, 2016, **237**, pp. 73–82
- [28] Das, M.C., Sandhu, P., Gupta, P., et al.: 'Attenuation of *Pseudomonas aeruginosa* biofilm formation by vitexin: A combinatorial study with azithromycin and gentamicin', *Sci. Rep.*, 2016, **6**, p. 23347
- [29] Aydin, R.S.T., Pulat, M.: '5-Fluorouracil encapsulated chitosan nanoparticles for ph-stimulated drug delivery: evaluation of controlled release kinetic', *J. Nanomater.*, 2012, **2012**, Article ID 313961
- [30] Ilk, S., Saglam, N., Ozgen, M., et al.: 'Chitosan nanoparticles enhances the anti-quorum sensing activity of kaempferol', *Int. J. Biol. Macromol.*, 2017, **94**, pp. 653–662
- [31] Silva, L.M., Hill, L.E., Figueiredo, E., et al.: 'Delivery of phytochemicals of tropical fruit by-products using poly (DL-lactide-co-glycolide) (PLGA) nanoparticles: synthesis, characterization, and antimicrobial activity', *Food. Chem.*, 2014, **165**, pp. 362–370
- [32] Hall, S., McDermott, C., Anoopkumar-Dukie, S., et al.: 'Cellular effects of pyocyanin, a secreted virulence factor of *Pseudomonas aeruginosa*', *Toxins*, 2016, **8**, p. 236
- [33] Ansari, M.A., Khan, H.M., Khan, A.A., et al.: 'Gum arabic capped-silver nanoparticles inhibit biofilm formation by multi-drug resistant strains of *Pseudomonas aeruginosa*', *J. Basic. Microbiol.*, 2014, **54**, (7), pp. 688–699
- [34] Nickzad, A., Deziel, E.: 'The involvement of rhamnolipids in microbial cell adhesion and biofilm development – an approach for control', *Lett. Appl. Microbiol.*, 2013, **58**, pp. 447–453
- [35] Prateeksha Singh, B.R., Shueb, M., et al.: 'Scaffold of selenium nanovectors and honey phytochemicals for inhibition of *Pseudomonas aeruginosa* quorum sensing and biofilm formation', *Front. Cell. Infect. Microbiol.*, 2017, **7**, p. 93